Received: 3 March 2021 | Revised: 7 April 2021 | Accepted: 26 April 2021

DOI: 10.1111/jne.12981

ORIGINAL ARTICLE

Journal of Neuroendocrinology WILEY

^{68}Ga-DOTATOC-PET/MRI and ^{11}C-5-HTP-PET/MRI are superior to ^{68}Ga-DOTATOC-PET/CT for neuroendocrine tumour imaging

Hiba Jawlakh[1] | Irina Velikyan[1] | Staffan Welin[2] | Anders Sundin[1]

[1]Department of Surgical Sciences, Radiology and Molecular Imaging, Uppsala University, Uppsala, Sweden

[2]Department of Medical Sciences, Uppsala University, Uppsala, Sweden

Correspondence
Anders Sundin, Department of Radiology and Molecular Imaging, Department of Surgical Sciences, Uppsala University, SE-753 31 Uppsala, Sweden.
Email: anders.sundin@radiol.uu.se

Abstract

The present study aimed to assess gadoxetate disodium contrast-enhanced (CE) positron emission tomography (PET)/magnetic resonance imaging (MRI) with ^{68}Ga-DOTATOC and ^{11}C-5-Hydroxy-tryptophan (^{11}C-5-HTP) in comparison with iodine CE ^{68}Ga-DOTATOC-PET/computed tomography (CT) for neuroendocrine tumour imaging. Detection rate and reader's confidence were evaluated for each separate image volume: CE-CT, CE-MRI including diffusion-weighted imaging, ^{68}Ga-DOTATOC-PET performed at PET/CT, ^{68}Ga-DOTATOC-PET performed at PET/MRI and ^{11}C-5-HTP-PET, and for the three combined hybrid examinations ^{68}Ga-DOTATOC-PET/MRI, ^{11}C-5-HTP-PET/MRI and ^{68}Ga-DOTATOC-PET/CT. In 11 patients, 255 lesions were depicted. ^{68}Ga-DOTATOC-PET performed at PET/MRI depicted 72.5%, ^{68}Ga-DOTATOC-PET performed at PET/CT depicted 62.7%, ^{11}C-5-HTP-PET depicted 68.2% and CE-CT depicted 53% of lesions. ^{68}Ga-DOTATOC-PET performed at PET/MRI ($P < 0.001$) and PET/CT ($P = 0.02$), ^{11}C-5-HTP-PET ($P < 0.001$) and MRI ($P < 0.001$) were superior to CT. ^{68}Ga-DOTATOC-PET/MRI and ^{11}C-5-HTP-PET/MRI detected 92.5% and 92% of lesions, respectively, and both outperformed ^{68}Ga-DOTATOC-PET/CT (65%) ($P < 0.001$). For liver metastasis imaging, MRI alone was unsurpassed ($P < 0.01$) and ^{68}Ga-DOTATOC-PET/MRI and ^{11}C-5-HTP-PET/MRI outperformed ^{68}Ga-DOTATOC-PET/CT ($P < 0.001$). For lymph node metastasis diagnosis, ^{68}Ga-DOTATOC-PET performed at PET/MRI and PET/CT and ^{11}C-5-HTP-PET detected 94%, 94% and 94% of lesions, respectively, and outperformed MRI and CE-CT alone ($P < 0.001$). For bone metastasis imaging, ^{68}Ga-DOTATOC-PET performed at PET/MRI and PET/CT and ^{11}C-5-HTP-PET performed equally well ($P = 0.05$) and better than MRI. Reader's confidence was better for ^{68}Ga-DOTATOC-PET/MRI and ^{11}C-5-HTP-PET/MRI than for ^{68}Ga-DOTATOC-PET/CT. The tumour maximum standardised uptake value and tumour-to-liver ratio were both approximately twice as high as for ^{68}Ga-DOTATOC than for ^{11}C-5-HTP. ^{68}Ga-DOTATOC-PET/MRI and ^{11}C-5-HTP-PET/MRI provided the highest detection rates and reader's confidence and were both superior to ^{68}Ga-DOTATOC-PET/CT, mainly because of the MRI component. The imaging contrast with ^{68}Ga-DOTATOC was superior to that of ^{11}C-5-HTP.

KEYWORDS
^{11}C-5-HTP, ^{68}Ga-DOTATOC, detection rate, neuroendocrine tumour, PET/CT, PET/MRI, SUV_{max}, tumour-to-background ratio

1 | INTRODUCTION

Neuroendocrine tumours (NETs) constitute a rare heterogeneous group of slow-growing and mainly well-differentiated tumours with potential secretory capacity, and may produce a variety of peptide hormones and biogenic amines.[1,2] In the USA, the incidence rate is approximately seven cases per 100,000 and year, and, according to a population-based study, the incidence rates increased by 6.4-fold between 1973 and 2012,[3,4] partly because of an improvement in diagnostic methods. NETs often arise sporadically and frequently originate in the gastrointestinal tract, including the pancreas (62%-67%), so-called gastroenteropancreatic NETs, and in the bronchopulmonary tract (22%-27%).[5] NETs are divided into functioning NETs that give rise to hormonal symptoms and non-functioning NETs that do not. The latter usually present with nonspecific symptoms, such as weight loss, stomach discomfort and pain because of the tumour's mass effect. Conversely, because of the hormonal symptoms, patients with functioning tumours present earlier. Because of the often vague initial symptoms, several years of patient and doctor delay is frequent, and 60% of patients present with metastasis.[1,6,7] Depending on their proliferation, Ki-67 index, NETs are graded as G1 (Ki-67 < 3%), G2 (Ki-67 3%-20%) and G3 (Ki-67 > 20%) and the G3 tumours are further divided into well-differentiated G3 NETs and poorly differentiated G3 neuroendocrine cancer.[8]

The wide variations of clinical NET-manifestations make the choice of diagnostic methods and imaging procedures challenging. Because surgery is the only curative of NET treatment, it is crucial to accurately localise the primary tumour and its extent and to detect regional and distant metastases to decide whether surgery is feasible. In locally advanced and/or metastatic disease, systemic treatment is instead initiated. This may be combined with debulking surgery and ablation of liver metastases, before which accurate imaging is also important.[9] Positron emission tomography combined with computed tomography (PET/CT) with ^{68}Ga-DOTA-somatostatin analogues (SSA) is the recommended modality for nuclear medicine imaging used in many centres for the management of NETs, especially in the diagnosis of well-differentiated NETs[10,11] with high sensitivity, usually > 90% and often even higher for well-differentiated G1 and G2 NETs with high somatostatin receptor (SSTR) expression.[12-15] A representative meta-analysis, including 17 papers, showed a pooled lesion-based sensitivity of 93% and a specificity of 85% for ^{68}Ga-DOTATOC-PET in the detection of NETs.[16] ^{68}Ga-DOTA-SSA-PET is especially valuable for visualising small lymph node metastases that often escape detection on CT and magnetic resonance imaging (MRI), or are falsely characterised as normal as a result of inadequate size criteria (short-axis diameter < 10 mm).[11] Similarly, bone metastases, often missed by CT, and are better detected by ^{68}Ga-DOTA-SSA-PET/CT with mean sensitivity and specificity ranging between 97%-100% and 92%-100%, respectively.[17,18]

PET/MRI has recently been introduced as a novel hybrid imaging tool, and several studies have evaluated the diagnostic accuracy of PET/MRI compared to PET/CT. A retrospective study that evaluated the impact of PET/MRI in different cancer types did not support the application of PET/MRI as an alternative to PET/CT in the clinical practice, but suggested that PET/MRI should be preferred over PET/CT in some cancers such as melanoma.[19]

Regarding NETs, there are few published reports with large heterogenicity in the study designs and patient populations, making it difficult to draw firm conclusion from their results. Some studies argue favourably for the use of PET/MRI, particularly in the detection of liver metastases, and the superiority of PET/MRI in those studies has been attributede to the MRI component because of its superiority to CT for detecting metastases to the liver, bone and brain.[11,19] MRI with diffusion-weighted sequences [diffusion-weighted imaging (DWI)] is sensitive for restricted diffusion in hypercellular malignant tumours,[20] and provides high lesion-to-background contrast, which, together with the lesion characterisation in the apparent diffusion coefficient map, facilitates lesion detection and helps to distinguish malignant from benign tumours. Moreover, because hepatocyte-specific MRI contrast media are available, this provides an additional advantage of MRI over CT for imaging of hepatic metastases.[21,22]

^{11}C-5-Hydroxy-tryptophan (^{11}C-5-HTP) is a PET-tracer that was developed and established as a primary nuclear medicine imaging method for NETs before the advent of ^{68}Ga-DOTA-SSA-PET/CT.[23] Its application is based on amine precursor uptake and decarboxylation (APUD) process where it accumulates in the neuroendocrine tumour cells (APUDomas) and undergoes decarboxylation yielding 5-hydroxy-tryptamine (serotonin), which is subsequently transported into vesicles of the NET cytoplasm.[24] Several comparative studies have shown that this is universally valid in NETs, except for poorly differentiated NETs, which show no or low uptake of ^{11}C-5-HTP.[25] However, a comparative PET study with ^{11}C 5-hydroxy-tryptophan and ^{68}Ga-DOTATOC has not previously been performed.

In the present prospective study, the combined hybrid imaging techniques PET/MRI with ^{68}Ga-DOTATOC and ^{11}C-5-HTP and PET/CT with ^{68}Ga-DOTATOC were compared in terms of detection rate and reader's confidence. In addition, the imaging capacity of the five individual components (CE-CT, CE-MRI, ^{68}Ga-DOTATOC in conjunction with PET/MRI, ^{68}Ga-DOTATOC in conjunction with PET/CT and ^{11}C-5-HTP-PET) were also investigated.

2 | MATERIALS AND METHODS

2.1 | Patients

Between August 2015 and April 2017, twelve consecutive adult patients, with histopathologically verified G1 and G2 NETs, except for one patient (patient 2), who was not biopsied, were prospectively included. One patient withdrew from the study and was excluded. The demographic and clinical characteristics are summarised in Table 1. The patients underwent a clinically indicated ^{68}Ga-DOTATOC-PET/CT. Whole-body ^{11}C-5-HTP-PET/MRI and whole-body ^{68}Ga-DOTATOC-PET/MRI were then performed for research purposes on the same day within 1-9 days (mean 2.6 days) of PET/CT. The study was approved by the local ethics committee (No. 2014/239) and written informed consent was obtained from all patients.

2.2 | Radiopharmaceutical production

Good manufacturing practice (GMP) compliant production of ^{11}C-5-HTP was conducted as reported previously.[26] Automated GMP production of ^{68}Ga-DOTATOC was performed on a synthesis platform (Modular PharmLab; Eckert & Ziegler, Seneffe, Belgium) using a disposable cassette system (C4-Ga68-PP) and pharmaceutical grade ^{68}Ge/^{68}Ga generator (GalliaPharm®; Eckert & Ziegler). The product was formulated in sterile saline and sterile-filtered in-line. The quality control in terms of radiochemical purity, chemical purity and quantity was conducted using high-performance liquid chromatography with ultraviolet- and radiodetectors connected in series.

2.3 | PET/CT and PET/MRI

Whole-body PET/CT ranging from the base of the skull to the proximal thighs was performed on a General Electric Discovery ST PET/CT scanner (GE Healthcare, Chicago, IL, USA) in patients 1-7 (Table 1) and on digital time-of-flight General Electric Discovery MI digital PET/CT scanner (GE Healthcare) in the remaining patients 8-11 (Table 1). The PET/CT and PET/MRI scanners were all cross-calibrated. Approximately 2 MBq kg^{-1} body weight ^{68}Ga-DOTATOC was administered i.v. as a bolus, and PET/CT was performed about 60 minutes following the injection. The Discovery ST and MI PET/CT scanners provided 15.7 cm and 20 cm axial coverage, respectively, and whole-body examinations were performed with 3 and 2 minutes PET-acquisition per bed position, respectively. The PET images were reconstructed with standard OSEM (ordered subset expectation maximisation) settings recommended by the manufacturer (three iterations/16 subsets and a 5-mm gaussian post-processing filter). A low-dose CT was performed for attenuation correction of the PET images (120 kV, auto mA 10-100 mA, noise index 28, rotation time 0.5 seconds, full spiral, slice thickness 3.75 mm, pitch 1.53:1). A diagnostic intravenously contrast-enhanced CT was performed in accordance with a clinical standard NET examination protocol used in the radiology department, including scanning of the liver in the late arterial contrast-enhancement phase and the neck, thorax, abdomen and pelvis in the venous phase (120 kV, auto-mA 85-560 mA, noise index 15, dose reduction 40%, rotation time 0.5 seconds, collimation 3.75 mm, pitch 0.95, reconstruction 0.6 mm transverse, 3-mm multi-reformatted transverse, coronal, sagittal). An iodine-based contrast medium (Iomeprol 400 mgI mL^{-1}; Bracco Imaging, Milan, Italy) 0.6 gI kg^{-1} body weight, was injected intravenously at 5 mL s^{-1}, utilising SmartPrep bolus tracking software (SmartPrep, München, Germany) to adjust the scanning in relation to contrast injection start to acquire the late arterial and venous contrast-enhancement phases, respectively.

PET/MRI with both ^{68}Ga-DOTATOC and ^{11}C-5-HTP were performed on a General Electric SIGNA PET/MRI 3.0 T system (Siemens Healthcare, Erlangen, Germany). The MRI component comprised a 60-cm bore 3 T magnet, gradient coils and transmit/receive body coils. The attenuation correction was performed using information from a LAVA-Flex scan (water only, fat only, in-phase and out-phase images). First, ^{11}C-5-HTP-PET/MRI was performed because of the shorter half-life of ^{11}C (20 minutes), followed by ^{68}Ga-DOTATOC-PET/MRI 4 hours later. The patients fasted for at least 4 hours before the examinations. Carbidopa (200 mg) was given perorally 1 hour before the injection of ^{11}C-5-HTP. Carbidopa is a peripheral aromatic L-amino acid decarboxylase enzyme inhibitor that decreases the decarboxylation rate for ^{11}C-5-HTP and, consequently, its excretion by the kidneys.[27] This provides a longer plasma half-life for 5-HTP, increasing its availability and thereby the tumour uptake. Approximately 5 MBq kg^{-1} bodyweight of ^{11}C-5-HTP was injected i.v. and PET acquisition was started 20 minutes later. An anti-peristaltic drug (Buscopan; Boehringer Ingelheim, Barcelona, Spain) was administered before the examinations to minimise the bowel movements and thereby reduce motion-induced MRI artifacts. The MRI sequences obtained concurrently with PET were: (i) transversal whole-body DWI with (b-values 0, 50, 800); (ii) transversal 3D LAVA flex sequence (water-only, fat-only, in-phase and out-phase images) performed during one breath-hold, including water-only, fat-only reconstructed by applying a two-point Dixon method; (iii) sagittal T1-weighted, T2-weighted and T2-STIR turbo spine echo of the cervical, thoracic and lumbar spine; (iv) coronal T1-weighted, T2-weighted turbo spin-echo of the lower abdomen and the pelvis; and (v) dynamic contrast-enhanced sequence in the transversal plane using a hepatocyte-specific contrast medium gadoxetate disodium (Primovist; Bayer-Schering Pharma, Berlin, Germany).

2.4 | Imaging analysis

The examinations were initially interpreted separately by two readers, one with basic radiological training and a senior consultant radiologist with 27 years of experience, who were blinded for all clinical and imaging information, except that the patients suffered from NET disease. In a second joint session, image analysis was performed by the two readers together in consensus. A workstation connected to the hospitals' picture archiving and communication system was used for image

TABLE 1 Patient characteristics and number of lesions detected on the five imaging volumes and on the three hybrid imaging modalities in each patient

Patient no.	Sex	Age (years)	Primary tumour	Metastases	Ki-67 (%)	^{68}Ga-DOTATOC-PET (PET/MRI)	^{68}Ga-DOTATOC-PET (PET/CT)	^{11}C-5-HTP-PET	MRI	CT	^{68}Ga-DOTATOC-PET/MRI	^{68}Ga-DOTATOC-PET/CT	^{11}C-5-HTP-PET/MRI
1	M	53	Pancreas (insulinoma)	Liver, LN	4	5	11	11	11	5	11	11	11
2	W	73	Pancreas (gastrinoma) MEN-1	LN	ND	2	2	0	0	0	2	2	0
3	M	51	Duodenal	0	3	1	1	0	1	1	1	1	1
4	M	74	Ileum, Pancreas	Mesentery	<2	3	3	3	2	2	3	3	3
5	W	68	Pancreas (MEN1)	Liver	<2	21	21	21	22	15	23	21	23
6	M	49	Small intestine	Liver, LN, PC	4	32	24	19	9	10	32	24	19
7	W	47	Small intestine	Liver, LN	3	ND	15	4	4	12	ND	19	9
8	W	51	Small intestine	Liver, LN, lung, breast, bone, pancreas	5	60	46	47	87	53	110	53	108
9	W	60	Small intestine	Liver, LN, PC, bone	4	48	41	64	28	34	59	40	75
10	W	68	Pancreas	Liver	7	5	5	4	7	5	7	5	7
11	W	55	Small intestine	Liver, LN	0.5	8	6	6	6	5	8	6	8

Abbreviations: LN, lymph node; M, man; MEN1, multiple endocrine neoplasia type 1; ND, not done; PC, peritoneal carcinomatosis; W, woman.

review. The five image volumes were analysed in the same manner in the separate and in the subsequent joint review session, with the reading performed in sequence and in the order: (i) contrast-enhanced CT; (ii) MRI including DWI and contrast-enhanced MRI of the liver; (iii) ^{68}Ga-DOTATOC-PET in conjunction with PET/CT; (iv) ^{68}Ga-DOTATOC-PET in conjunction with PET/MRI; and (v) ^{11}C-5-HTP-PET in conjunction with PET/MRI. All lesions depicted on PET were checked for morphological correlation on CT/MR. Because of the sequential review, the readers were not blinded for the findings on the first imaging volume (CT) when preceding to the second volume, and so forth.

For each of the five image volumes, the evaluation was performed in two steps: first, to determine whether the respective modality depicted a lesion or not (detection/ no detection) and, second, by scoring the reader's confidence for lesion depiction according to a five-point scale from 0 to 4 as: 0, not depicted; 1, low suspicion; 2, moderate suspicion; 3, strong suspicion; and 4, definite tumour finding. Lesions depicted by the morphological modalities (CT/MRI) achieved score 4 only when they showed a typical unequivocal appearance. Lesions depicted by PET achieved score 4 only when morphological correlation on CT/MRI was verified. Because patient 7 (Table 1) did not undergo ^{68}Ga-DOTATOC-PET/MRI, including CE-MRI and DWI-MRI, data from this patient were not included in the analysis of the detection rate and reader's confidence.

Furthermore, to assess the tumour uptake in the different PET-volumes, the maximum standardised uptake value (SUV_{max}) for selected lesions with the highest tracer uptake was obtained by drawing spherical volumes of interest of variable diameter to include the respective tumours. For each of the three PET-volumes, the SUV_{max} was measured in three lesions in the organs: liver, lymph nodes, bone, pancreas, intestine, lung, peritoneum and breast. To calculate the tumour-to-background contrast in the different PET-volumes, the SUV_{mean} in normal liver was obtained by drawing a 2 cm diameter region of interest in the posterior part of the right liver lobe, and the tumour-to-normal liver ratio (TLR) was calculated by dividing the tumour SUV_{max} by the normal liver SUV_{mean}. PET measurements were obtained from all patients, including patient 7.

It was not possible in this type of study to achieve histopathological verification for every depicted tumour lesion. Therefore, all lesions diagnosed in at least one of the five image volumes constituted the 'gold standard'. For a few selected lesions, when needed, verification of the image findings was obtained by correlation with subsequent serial imaging follow-up during at least one year.

2.5 | Statistical analysis

Data were compiled in Excel (Microsoft Corp., Redmond, WA, USA). R, version 4.0.2 (R Foundation for Statistical Computing, Vienna, Austria) was used for statistical analysis. A chi-squared test of independence and Fisher's exact test (when the lesion number was < 5 per cell) were applied to evaluate the difference in the detection rates, as well as the reader's confidence between the five imaging volumes and the three hybrid modalities. Both multiple analyses and pairwise comparisons were performed. The Wilcoxon signed-rank test was used to compare SUV_{max} on ^{68}Ga-DOTATOC-PET in conjunction with PET/CT, ^{68}Ga-DOTATOC-PET in conjunction with PET/MRI and on ^{11}C-5-HTP-PET/MRI. $P < 0.05$ was considered statistically significant.

3 | RESULTS

All patients underwent all of the examinations successfully, except for patients 4 and 6 (Table 1), who did not undergo CE-MRI, and patient 7 (Table 1), who did not undergo ^{68}Ga-DOTATOC-PET/MRI. Because the results of MRI were based on the combined findings from CE-MRI and DWI-MRI, patients 4 and 6 could still be included in the comparison between the modalities.

3.1 | The five morphological and functional image volumes: Detection rate

The number of diagnosed lesions and detection rates for the five imaging volumes and on the three PET/CT and PET/MRI hybrid imaging sets are summarised in Table 2. In total, 255 lesions were depicted, of which 187 (73.3%) were liver metastases, 17 (6.6%) were lymph node metastases, 19 (7.4%) were bone metastases, 21 (8.2%) were peritoneal metastases and 11 (4.3%) were lesions detected in other anatomical positions, including one lung metastasis, two breast metastases, and eight primary tumours comprising six small-intestinal NETs and two pancreatic NETs.

^{68}Ga-DOTATOC-PET in conjunction with PET/MRI, visualised most lesions (72.5%), followed by ^{11}C-5-HTP-PET (68.2%), MRI (67.8%) and ^{68}Ga-DOTATOC-PET in conjunction with PET/CT (62.7%), and were all superior to CT ($P < 0.001$, $P = 0.02$, $P < 0.001$, $P < 0.001$), which, detected the least lesions (53%). ^{68}Ga-DOTATOC-PET in conjunction with PET/MRI performed better than in conjunction with PET/CT ($P = 0.01$). Patients 2 and 3 were negative on ^{11}C-5-HTP-PET (Figures 1 and 2).

MRI was superior to the other four imaging modalities ($P < 0.01$) with respect to detecting liver metastases (85%), followed by ^{68}Ga-DOTATOC-PET in conjunction with PET/MRI (68.4%) and ^{11}C-HTP-PET (60.4%). ^{68}Ga-DOTATOC-PET in conjunction with PET/CT and CT visualised 53.45% and 48.6% of the lesions, respectively. ^{68}Ga-DOTATOC-PET in conjunction with PET/MRI was better than ^{68}Ga-DOTATOC-PET at PET/CT ($P = 0.02$) and ^{68}Ga-DOTATOC-PET in conjunction with PET/MRI and ^{11}C-5-HTP-PET were better than CT ($P = 0.001$ and $P = 0.02$, respectively).

Lymph node metastases were equally well detected by ^{68}Ga-DOTATOC-PET in conjunction with PET/MRI and ^{68}Ga-DOTATOC-PET in conjunction with PET/CT, as well as by ^{11}C-5-HTP-PET (94%), which all were superior to MRI ($P < 0.001$) and CT ($P < 0.001$), which detected 17.6% (MRI) and 41% (CT) of lesions, respectively.

Bone metastases were predominantly depicted on ^{11}C-5-HTP-PET (89.4%), followed by ^{68}Ga-DOTATOC-PET in conjunction with

TABLE 2 Number of lesions detected on each of the five imaging volumes and on the three hybrid imaging volumes

	^{68}Ga-DOTATOC-PET (PET/MRI)	^{68}Ga-DOTATOC-PET (PET/CT)	^{11}C-5-HTP PET	MRI (CE + DWI)	CT	^{68}Ga-DOTATOC-PET/MRI	^{68}Ga-DOTATOC-PET/CT	^{11}C-5-HTP-PET/MRI
All lesions	185 (72.5%)	160 (62.7%)	174 (68.2%)	173 (67.8%)	130 (53%)	256 (92.5%)	166 (65%)	255 (92%)
Liver metastases	128 (68.4%)	100 (53.5%)	113 (60.4%)	159 (85%)	91 (48.6%)	179 (95.7%)	106 (56.6%)	173 (92.5%)
Lymph node metastases	16 (94%)	16 (94%)	16 (94%)	3 (17.6%)	7 (41%)	16 (94%)	16 (94%)	16 (94%)
Bone metastases	12 (63%)	17 (89.4%)	12 (63%)	4 (21%)	0 (0%)	12 (63%)	17 (89.4%)	12 (63%)
Peritoneal metastases	18 (85.7%)	21 (100%)	19 (90.4%)	4 (19%)	19 (90.4%)	18 (85.7%)	21 (100%)	19 (90.4%)
Other locations	11 (100%)	11 (100%)	9 (81.8%)	3 (27.2%)	8 (72.7%)	11 (100%)	11 (100%)	10 (91%)

Note: Detection rate (%).

FIGURE 1 73-year-old woman with a metastatic pancreatic neuroendocrine tumour (NET) (Patient 2). A + B, Maximum intensity projection, anterior view. A, ^{68}Ga-DOTATOC-PET shows a lymph node metastasis (black arrow). B, On ^{11}C-5-HTP-PET, no lesions are detected. C, Transaxial fused ^{68}Ga-DOTATOC-PET/MRI in liver level shows a pancreatic NET (long white arrow), tracer uptake in the gastric wall (short white arrow) and physiological tracer uptake in the uncinate process of the pancreas (white star). D, Transaxial ^{11}C-5-HTP-PET/MRI fusion shows no lesions

FIGURE 2 Maximum intensity projection, anterior view. A, ^{68}Ga-DOTATOC-PET image shows a duodenal neuroendocrine tumour (NET) (black arrow) in a 51-year old man (Patient 3). B, ^{11}C-5-HTP-PET shows no lesions

PET/MRI (63%) and ^{68}Ga-DOTATOC-PET in conjunction with PET/CT (63%), although this was only borderline significant (P = 0.05). This is illustrated in patient 9 in Figure 3. ^{68}Ga-DOTATOC-PET in

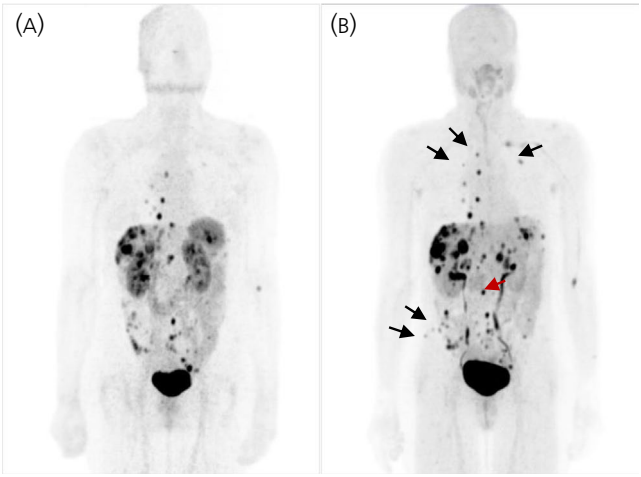

FIGURE 3 Maximum intensity projection, anterior view. A, ^{68}Ga-DOTATOC-PET on a 60-year-old woman with metastatic small intestinal neuroendocrine tumour (NET) (Patient No 9). B, ^{11}C-5-HTP-PET shows more lesions [lymph node metastases (red arrow) and bone metastases (black arrows)] detected with ^{11}C-5-HTP compared to ^{68}Ga-DOTATOC

conjunction with PET/MRI ($P < 0.01$) and PET/CT ($P < 0.01$), as well as ^{11}C-5-HTP-PET ($P < 0.001$), were all superior to MRI. However, 21% of lesions were visualised on MRI, which was better than CT ($P = 0.03$), which missed all bone metastases.

^{68}Ga-DOTATOC-PET in conjunction with PET/CT detected all peritoneal metastases followed by ^{11}C-5-HTP-PET and CT, which performed equally well (90.4%), and ^{68}Ga-DOTATOC-PET in conjunction with PET/MRI (85.7%). These four modalities were superior to MRI ($P < 0.001$), which detected only 19% of lesions.

3.2 | The five morphological and functional image volumes: Reader's confidence

Lesions scored 2 points or more were considered as positive findings and were included in the analysis of the reader's confidence for lesion detection. Overall, the reader's confidence was similar for all five imaging volumes when all metastases were included ($P = 0.5$) and for bone metastases ($P = 0.2$) (Table 3). For liver metastases detection, the reader's confidence was better for MRI than for ^{68}Ga-DOTATOC-PET in conjunction with PET/MRI ($P = 0.001$) and PET/CT ($P < 0.001$), and also better than for ^{11}C-5-HTP-PET ($P < 0.001$) (Table 3). ^{68}Ga-DOTATOC-PET in conjunction with PET/MRI and PET/CT, as well as ^{11}C-5-HTP-PET, showed similar results ($P > 0.05$). The reader's confidence for detecting lymph node metastases was similar for ^{68}Ga-DOTATOC-PET in conjunction with PET/MRI and PET/CT, and also for ^{11}C-5-HTP-PET ($P > 0.05$), but were for all three imaging volumes higher than that for CT ($P < 0.001$). For peritoneal metastases, ^{68}Ga-DOTATOC-PET in conjunction with PET/MRI ($P = 0.01$) and ^{11}C-5-HTP-PET ($P = 0.01$) were superior to MRI. ^{68}Ga-DOTATOC-PET, in conjunction with PET/CT, showed a higher reader's confidence than that for ^{68}Ga-DOTATOC-PET in conjunction with PET/MRI ($P < 0.001$) and ^{11}C-5-HTP-PET ($P = 0.01$).

3.3 | The hybrid imaging modalities: Detection rate

Detection rates for the three hybrid imaging combinations are shown in Table 3. Overall, PET/MRI with ^{68}Ga-DOTATOC and ^{11}C-5-HTP showed similar detection rates, at 92.5% and 92%, respectively, and were both superior to ^{68}Ga-DOTATOC-PET/CT (65%) ($P < 0.001$). Liver metastases were detected similarly well by ^{68}Ga-DOTATOC-PET/MRI (95.7%) and ^{11}C-5-HTP-PET/MRI (92.5%) ($P = 0.1$), and both performed better than ^{68}Ga-DOTATOC-PET/CT (56.6%) ($P < 0.001$). All three hybrid modalities detected the same number of lymph node metastases (94%).^{68}Ga-DOTATOC-PET/MRI, ^{68}Ga-DOTATOC-PET/CT and ^{11}C-5-HTP-PET/MRI performed equally well for bone metastases ($P = 0.1$) and peritoneal metastases ($P = 0.2$).

3.4 | The hybrid imaging modalities: Reader's confidence

In the overall comparison of all lesions, the reader's confidence was higher for ^{68}Ga-DOTATOC-PET/MRI than for ^{11}C-5-HTP-PET/MRI ($P = 0.01$) and higher for both ^{68}Ga-DOTATOC-PET/MRI ($P = 0.01$) and ^{11}C-5-HTP-PET/MRI ($P < 0.001$) than for ^{68}Ga-DOTATOC-PET/CT. For detection of liver metastases, the reader's confidence was higher for ^{68}Ga-DOTATOC-PET/MRI ($P = 0.005$) and ^{11}C-5-HTP-PET/MRI ($P = 0.001$) than on ^{68}Ga-DOTATOC-PET/CT but similar to that for ^{68}Ga-DOTATOC-PET/MRI and ^{11}C-5-HTP-PET/MRI ($P = 0.9$) (Table 3). For peritoneal metastases the reader's confidence was higher for ^{68}Ga-DOTATOC-PET/CT than for ^{68}Ga-DOTATOC-PET/MRI ($P = 0.002$) and ^{11}C-5-HTP-PET/MRI ($P = 0.01$). The three hybrid imaging modalities showed similar reader's confidence for detection of lymph node metastases and bone metastases ($P = 0.7$) and ($P = 0.05$), respectively.

3.5 | Quantitative analysis: PET measurements

The tumour uptake of ^{68}Ga-DOTATOC was similar on PET in conjunction with PET/MRI and in conjunction with PET/CT: SUV_{max} (mean ± SD) 22.8 ± 17.2 and 22.0 ± 15.4, respectively ($P = 0.6$). This was almost twice as high as for ^{11}C-5-HTP-PET, with tumour SUV_{max} (mean ± SD) 12.0 ± 7.5 ($P < 0.001$) (Figure 4). A higher tumour-to-liver ratio was found on ^{68}Ga-DOTATOC-PET/MRI 7.0 ± 4.6 ($P < 0.001$) and ^{68}Ga-DOTATOC-PET/CT 7.6 ± 4.8 ($P < 0.001$) than on ^{11}C-5-HTP-PET/MRI 3.3 ± 2.0 (Figure 5). In liver metastases, the ^{68}Ga-DOTATOC uptake (mean ± SD) SUV_{max} was 27.5 ± 22.5 and 24.7 ± 18.5 on PET/MRI and PET/CT, respectively, which was higher than that on ^{11}C-5-HTP-PET/MRI 13.0 ± 6.4 ($P < 0.001$) (Figure 4). Also, the ^{68}Ga-DOTATOC tumour-to-liver ratio for liver metastases on PET/MRI (mean ± SD) (9.1 ± 6.2) and on PET/CT (8.7 ± 5.0) was higher than for ^{11}C-5-HTP (3.6 ± 1.6) ($P < 0.001$) (Figure 5). The differences in PET tracer uptake were also found for the other types of metastases (Figures 4 and 5 and Table 4), except for peritoneal metastases and bone metastases, in which SUV_{max} and tumour-to-liver

TABLE 3 The reader's confidence for lesion detection on the five imaging volumes and the three hybrid imaging modalities

Score	^{68}Ga-DOTATOC-PET (PET/MRI)	^{68}Ga-DOTATOC-PET (PET/CT)	^{11}C-5-HTP PET	MRI (CE + DWI)	CT	^{68}Ga-DOTATOC-PET/MRI	^{68}Ga-DOTATOC-PET/CT	^{11}C-5-HTP-PET/MRI
All lesions								
2 p	6	6	7	10	10	14	11	16
3 p	62	48	60	57	32	105	49	112
4 p	117	104	107	106	76	117	105	107
Liver metastases								
2 p	3	2	3	9	4	12	7	12
3 p	22	18	16	53	23	64	19	67
4 p	103	79	94	97	63	103	79	94
Lymph node metastases								
2 p	0	0	0	0	3	0	0	0
3 p	13	11	13	1	0	13	11	13
4 p	3	5	3	2	4	3	5	3
Bone metastases								
2 p	2	2	1	1	0	2	2	2
3 p	6	10	11	2	0	6	10	11
4 p	4	0	4	0	0	4	0	4
Peritoneal metastases								
2 p	1	2	2	0	0	0	2	2
3 p	13	5	13	0	8	14	5	13
4 p	4	14	4	4	6	4	14	4
Other locations								
2 p	0	0	0	0	3	0	0	0
3 p	8	7	8	0	1	8	4	8
4 p	3	4	2	4	3	3	7	2

Note: For each imaging volume, the number of lesions is shown for each score, for all lesions and separately for different types of metastases. The number of lesions were scored with 2, 3 and 4 points (p).
Abbreviations: CE, contrast-enhanced, DWI, diffusion-weighted imaging.

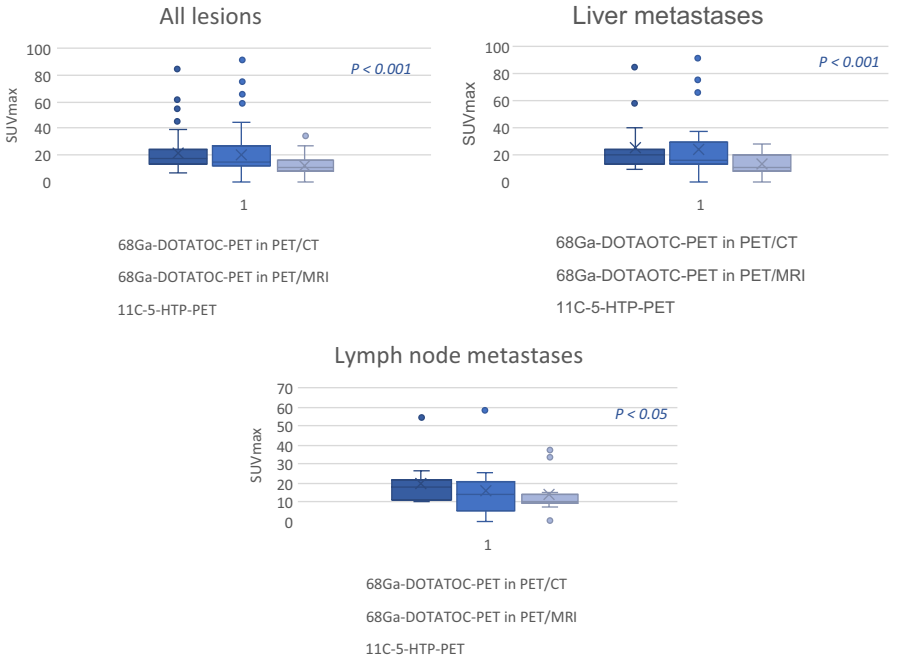

FIGURE 4 Box plot of the maximum standardised uptake values (SUV_{max}, *y*-axis) measured on ^{68}Ga-DOTATOC in conjunction with PET/CT and PET/MRI and on ^{11}C-5-HTP-PET/MRI

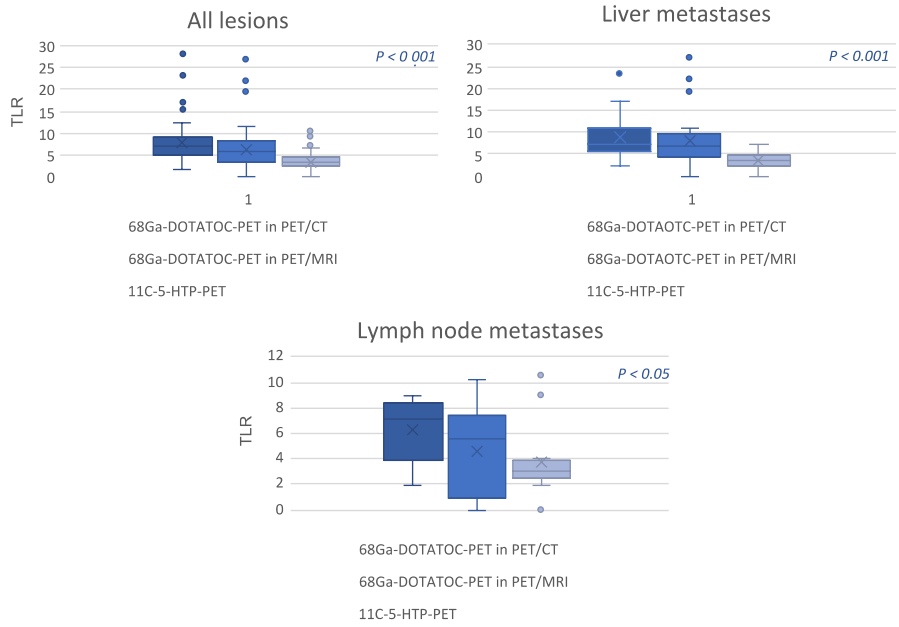

FIGURE 5 Box plot of the tumour-to-liver ratio (TLR, *y*-axis) measured on ^{68}Ga-DOTATOC in conjunction with PET/CT and PET/MRI and on ^{11}C-5-HTP-PET

ratio were similar, despite the values for ^{68}Ga-DOTATOC being more than twice those for ^{11}C-5-HTP (Table 4).

4 | DISCUSSION

Whole-body imaging of NET patients has widely expanded as a result of its essential role in the diagnosis and management of NETs. The present study demonstrates that the overall tumour detection rate and reader's confidence on PET/MRI with ^{68}Ga-DOTATOC and ^{11}C-5-HTP were superior to that of ^{68}Ga-DOTATOC-PET/CT. However, for liver metastases, MRI as a separate imaging method showed superior results, exceeding those on ^{68}Ga-DOTATOC-PET, ^{11}C-5-HTP-PET and CE-CT (Figure 6). The vast majority of published comparisons of PET/CT and PET/MRI with ^{68}Ga-DOTA-SSA-preparations have been performed following a single tracer injection, where, generally, a clinical PET/CT has preceded the PET/MRI study examination.[28-31] This means that these comparisons have favoured PET/MRI because of the considerably longer time provided for tracer accumulation in the tumours. By contrast, in the present study, PET/CT and PET/MRI were performed after separate tracer injections, and with a similar uptake time before scanning, aiming to provide a non-biased comparison in this aspect and constituting a major methodological advantage compared to several previous studies.[28-31] Also, PET/CT and PET/MRI were performed close in time, being only 1-9 days apart.

TABLE 4 Tumour uptake (mean ± SD) of ^{68}Ga-DOTATOC and ^{11}C-5-HTP on PET/CT and PET/MRI

	^{68}Ga-DOTATOC- PET/MR	^{68}Ga-DOTATOC- PET/CT	^{11}C-5-HTP- PET/MR
SUV_{max}			
All metastases	22.8 ± 17.2	22.03 ± 15.4	12.0 ± 7.5
Liver metastases	27.5 ± 22.5	24.7 ± 18.5	13.0 ± 6.4
Lymph node metastases	20.1 ± 13.8	19.7 ± 11.1	13.8 ± 10.0
Bone metastases	17.0 ± 10.2	18.7 ± 12.5	7.5 ± 3.2
Peritoneal metastases	12.6 ± 4.2	11.6 ± 3.5	9.4 ± 2.6
Metastases in other locations	23.7 ± 13.0	25.3 ± 16.5	10.8 ± 8.7
TLR			
All metastases	7.0 ± 4.6	7.6 ± 4.8	3.3 ± 2.0
Liver metastases	9.1 ± 6.2	8.7 ± 5.1	3.6 ± 1.6
Lymph node metastases	5.7 ± 2.4	6.3 ± 2.3	3.7 ± 2.7
Bone metastases	5.6 ± 2.8	7.5 ± 4.8	2.2 ± 0.8
Peritoneal metastases	5.0 ± 4.2	4.8 ± 1.3	2.7 ± 0.7
Metastases in other locations	5.7 ± 3.1	8.3 ± 7.1	3.0 ± 2.3

Abbreviations: SUV_{max}, maximum standardised uptake value; TRL, tumour-to-liver ratio.

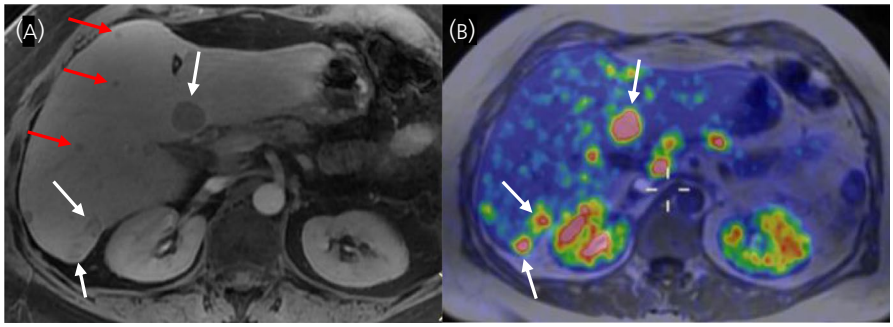

FIGURE 6 Showing the better detection of liver metastases on MRI than on ^{68}Ga-DOTATOC-PET. The combined PET/MRI hybrid imaging increases the lesion detection and the reader's confidence compared to each imaging modality alone. A, Transaxial contrast-enhanced MRI, 20 minutes after the administration of a hepatocytespecific contrast medium, shows three of the liver metastases which also were detected on ^{68}Ga-DOTATOC-PET (white arrows) and three of the liver metastases which were only detected on MRI (red arrows). B, Transaxial fused ^{68}Ga-DOTATOC-PET/MRI shows high uptake in the same lesions as in a (white arrows) but several of the lesions diagnosed on MRI show no ^{68}Ga-DOTATOC uptake

As a singular imaging method, ^{68}Ga-DOTATOC-PET performed in conjunction with PET/MRI provided the highest overall tumour detection rate (72.5%) and outperformed ^{11}C-5-HTP-PET (68.2%), MRI (67.8%) and contrast-enhanced CT, the latter of which not unexpectedly showed the worst performance (53%). By contrast to our results, Ruf et al[32] reported a higher detection rate for CE-CT (77.1%) than for ^{68}Ga-DOTATOC-PET (72.8%), which may be partly explained by the more heterogeneous patient cohort in their study. Another retrospective study comparing ^{68}Ga-DOTATOC-PET/CT and whole-body MRI noted a higher detection rate for MRI (91%) than for ^{68}Ga-DOTATOC-PET (64%) and CE-CT (81%).[33] However, some NETs in that study were SSTR-negative, and when only SSTR-positive NETs were evaluated, the detection rate was higher for ^{68}Ga-DOTATOC-PET than for CT, although still lower than for MRI. In the present study, the detection rates were better on hybrid ^{68}Ga-DOTATOC-PET/MRI (92.5%) and ^{11}C-5-HTP-PET/MRI (92%) than on ^{68}Ga-DOTATOC-PET/CT (65%). This was in contrast to Sawicki et al,[28] who reported almost similar detection rates for ^{68}Ga-DOTATOC-PET/CT and ^{68}Ga-DOTATOC-PET/MRI, 93.9% and 92.9%, respectively. However, also in their study, a higher number of correctly classified NETs was found on ^{68}Ga-DOTATOC-PET/MRI than on ^{68}Ga-DOTATOC-PET/CT. Most of the lesions missed on ^{68}Ga-DOTATOC-PET/CT in the present study were liver metastases that neither ^{68}Ga-DOTATOC-PET, nor CT could visualise, which may explain the difference in detection rates between the three modalities.

The present study includes the first PET imaging comparison between ^{11}C-5-HTP and ^{68}Ga-DOTATOC, showing that PET/MRI with ^{68}Ga-DOTATOC and ^{11}C-5-HTP achieved similar lesion detection rates, both overall and for the various types of metastases. However, as a singular imaging method, ^{68}Ga-DOTATOC-PET was superior to ^{11}C-5-HTP-PET. Interestingly, the lesion visualisation results with ^{11}C-5-HTP-PET and ^{68}Ga-DOTATOC-PET varied between patients,

in the sense that, in some subjects, one tracer was superior and vice versa. A notable finding in the present study was that ^{11}C-5-HTP-PET/MRI detected additional bone metastases that were not visualised by either ^{68}Ga-DOTATOC-PET/CT or ^{68}Ga-DOTATOC-PET/MRI. This illustrates the advantage of having the alternative tracer ^{11}C-5-HTP available, especially for staging of occasional patients with low-grade (G1-2) tumours that show low or no ^{68}Ga-DOTATOC uptake. Conversely, two of our patients (patients 2 and 3) were ^{11}C-5-HTP negative. A similar result was found by Örlefors et al,[24] who reported ^{11}C-5-HTP-negativity in two out of 38 patients, with a pancreatic neuroendocrine cancer and a non-functioning pancreatic NET, respectively. In a more recent study by Örlefors et al,[34] ^{11}C-5-HTP-PET was negative in six out of 38 patients undergoing surgical resection (two non-functioning pancreatic NET, two insulinomas, two pancreatic NETs in MEN-I patients). These findings demonstrate that the APUD-system is not always expressed and may be less well-developed, or down-regulated, in some tumours. Unfortunately, the data did not allow us to assess any relation between ^{11}C-5-HTP positivity/negativity and tumour proliferation (Ki-67 index), for which additional studies are needed. Nevertheless, ^{11}C-5-HTP constitutes a valuable problem-solving tracer in the few patients who are harbouring tumours escaping detection by ^{68}Ga-DOTATOC-PET.

Before the era of PET/CT with ^{68}Ga-DOTA-somatostatin analogues, ^{11}C-5-HTP, and ^{18}F-DOPA mainly constituted the PET-tracers for NET imaging and were found to be superior to somatostatin receptor scintigraphy using ^{111}In-octreotide,[24,25,34,35] detecting additional tumours, particularly small lesions and primary tumours that were missed on morphological imaging. In accordance with the literature,[24] ^{11}C-5-HTP-PET was found to detect more lesions than CE-CT in the present study.

Concerning the reader's confidence, this was similar for the five separate image volumes. However, the hybrid imaging modalities ^{68}Ga-DOTATOC-PET/MRI and ^{11}C-5-HTP-PET/MRI showed better reader's confidence both for overall tumour detection and for diagnosing liver metastases. This may be partly related to the larger number of lesions detected on MRI than on CT, and also because morphological correlation on MRI was required to achieve a four-point score, according to our evaluation criteria.

Because the detection rate for liver metastases on ^{68}Ga-DOTATOC-PET/CT has previously been shown lower than on MRI,[36] and because the liver is the main organ for distant NET metastases, the combination of CE-MRI together with ^{68}Ga-DOTATOC PET/CT has been suggested.[31,36,37] We found MRI to be superior to the other imaging modalities with a detection rate of 85%. This is in line with Hope et al,[30] who demonstrated higher sensitivity for CE-MRI (99%) and DWI-MRI (83%) than for ^{68}Ga-DOTATOC-PET in conjunction with PET/CT (63%) and PET/MRI (61%). Also, in accordance with our findings, and not unexpectedly, CE-CT alone showed the lowest sensitivity, at merely 46%. DWI-MRI provides higher tumour-to-background contrast, but is still less sensitive than gadoxetate-enhanced MRI that may visualise small sub-centimeter liver lesions below the resolution limit of PET, or which lack sufficient SSTR expression[22]; accordingly, the combination of DWI-MRI and gadoxetate-enhanced MRI previously showed a higher accuracy than each imaging technique alone.[21]

For the hybrid modalities, and in line with previous studies, ^{68}Ga-DOTATOC-PET/MRI was found to be superior to ^{68}Ga-DOTATOC-PET/CT.[38,39] For lymph node metastases, hybrid imaging by ^{68}Ga-DOTATOC-PET/MRI, ^{68}Ga-DOTATOC-PET/CT and ^{11}C-5-HTP-PET/MRI yielded similar detection rates and reader's confidence and they were superior to MRI and CT alone. This in line with the literature,[28,30] although Berzaczy et al[31] by contrast reported a higher sensitivity for ^{68}Ga-DOTATOC-PET/MRI (100%) than for ^{68}Ga-DOTATOC-PET/CT (78.6%). This also illustrates the advantage of functional modalities to provide means for lesion detection and characterisation,[10] whereas, on CT/MRI, small lymph node metastases, with short-axis < 1 cm, may be missed or misinterpreted as normal.

Similarly, the three hybrid modalities, ^{68}Ga-DOTATOC-PET/MRI, ^{68}Ga-DOTATOC-PET/CT and ^{11}C-5-HTP-PET/MRI, performed equally well in the detection of both bone metastases and peritoneal metastases, and differences were only noted between the five separate imaging volumes.

Because most bone metastases are usually asymptomatic, they generally remained undetected on CT and the development of functional imaging with ^{68}Ga-DOTA-SSAs has considerably improved their visualisation.[40,41] Our detection rates for bone metastases on ^{11}C-5-HTP-PET and on ^{68}Ga-DOTATOC-PET in conjunction with both PET/CT and PET/MRI were much higher than on both CT and MRI, which is in line with earlier studies comparing ^{68}Ga-DOTATOC-PET/CT and CT.[38,42,43] In the literature, MRI has been described as the most sensitive method for detecting bone metastases with up to 100% sensitivity, and DWI-MRI has shown high sensitivity for detection of non-NET bone metastases from other tumours than NETs.[44,45] Consistent with previous reports, we found MRI to be superior to CT, which, in the present study, notably missed all bone metastases.

DWI-MRI and gadolinium-enhanced MRI have in previous studies been reported as being superior to CT for the detection of peritoneal metastases and overall staging because of the better soft-tissue contrast. Particularly, small peritoneal metastases are missed on CT, and, for peritoneal tumours < 1 cm, less sensitivity on CT (25%-50%) was reported compared to 85%-95% when tumours of all sizes were considered.[46,47] In a previous comparison between CE-CT and ^{68}Ga-DOTATOC-PET/CT, more peritoneal metastases were detected on PET/CT (78%) than on CE-CT (38%) alone, underlining the efficacy of hybrid imaging.[48] Conversely, in the present study, CT was found to be superior to MRI and, furthermore, the reader's confidence was better for ^{68}Ga-DOTATOC-PET/CT than for PET/MRI with ^{68}Ga-DOTATOC and ^{11}C-5-HTP. These findings are not easily explained, although parameters to be considered are the higher tumour uptake of ^{68}Ga-DOTATOC, typically twice as high as that for ^{11}C-5-HTP, with, consequently, a clearly better tumour-to-background contrast for ^{68}Ga-DOTATOC, and a less physiological normal tissue uptake of ^{11}C-5-HTP than that of ^{68}Ga-DOTATOC in the abdomen, creating more favourable conditions for the former tracer. Furthermore,

it cannot be ruled out that, in the assessment of these lesions, the recent comparison of CE-CT and ^{68}Ga-DOTATOC[48] may have created a training situation, particularly for CT detection of peritoneal metastases.

^{68}Ga-DOTATOC showed very high tumour accumulation, clearly exceeding that of ^{11}C-5-HTP, typically with a SUV_{max} twice as high as that for ^{11}C-5-HTP. Probably even more essential, given the high abundance of liver metastases in NET patients, was the higher TLR for ^{68}Ga-DOTATOC than for ^{11}C-5-HTP, facilitating detection of liver metastases. The advantage of ^{11}C-5-HTP-PET is its capacity to visualise NETs regardless of the degree of SSTR expression. However, because our cohort was limited to well-differentiated GI and low G2 NETs, the efficacy of ^{11}C-5-HTP in NETs with a higher proliferation rate, for which ^{11}C-5-HTP may be less sensitive,[24] could not be investigated and needs to be explored further in future studies.

An inherent limitation in this type of study is the lack of surgical and pathological confirmation of the image findings and, consequently, of a 'gold standard'. Because clinical and ethical standards of patient management exclude repeated and multiple biopsies for histopathological confirmation, a modified standard of reference was applied based on the combined imaging results from all modalities and on clinical and imaging follow-up for at least 1 year. Furthermore, this limited cohort of patients harboured well-differentiated GI and low G2 NETs, but no high-grade tumours. Another limitation is that some patients underwent examinations on PET/CT scanners with different PET components. Thus, 7/11 (64%) of patients underwent PET/CT on the older Discovery ST and 4/11 (36%) on the new Discovery MI PET/CT scanner. This most likely explains the lower detection rates for PET performed in conjunction with PET/CT than in conjunction with PET/MRI, equipped with the same PET-component as the Discovery MI PET/CT scanner.

The imaging evaluation was strictly blinded in the sense that each of the five imaging volumes was interpreted separately, although the reading was performed sequentially, which may have introduced a bias. A drawback, especially concerning ^{11}C-5-HTP, is the complicated synthesis, which limits its use to a few centres. The novelty of the present study was the head-to-head comparison of the PET tracers ^{11}C-5-HTP and ^{68}Ga-DOTATOC, which has previously not been performed, and, in addition, all comparisons were performed for PET/CT and PET/MRI following separate tracer injections, rather than performing PET/MRI as an add on following PET/CT after one administration.

In conclusion, a high detection rate and reader's confidence were found for ^{68}Ga-DOTATOC-PET/MRI and ^{11}C-5-HTP-PET/MRI, implying that they should be preferred over PET/CT for NET imaging as a result of the higher accuracy of DWI and CE-MRI, particularly for detecting metastases to liver and bone. Because of the limited number of patients in the present study, further comparative trials in larger cohorts, also including also high G2 and G3 NET patients, are warranted.

CONFLICT OF INTERESTS

The authors declare that they have no conflicts of interest.

AUTHOR CONTRIBUTIONS

Hiba Jawlakh: Data curation; Formal analysis; Methodology; Writing - original draft; Writing - review & editing. **Irina Velikyan:** Methodology; Writing - review & editing. **Staffan Welin:** Writing - review & editing. **Anders Sundin:** Conceptualisation; Data curation; Investigation; Methodology; Project administration; Supervision; Writing - review & editing.

ETHICAL STATEMENT

All patients provided their informed consent. The study was approved by the regional ethics committee. All procedures performed were in accordance with the 1964 Helsinki Declaration and its later amendments or comparable ethical standards.

PEER REVIEW

The peer review history for this article is available at https://publons.com/publon/10.1111/jne.12981.

ORCID

Anders Sundin https://orcid.org/0000-0002-2214-6217

REFERENCES

1. Jankowski JAZ. Neuroendocrine tumors. *Gastrointestinal Oncology a Critical Multidisciplinary Team Approach*. London: Blackwell Publishers; 2008.
2. Kilickap S, Hayran KM. Epidemiology of neuroendocrine tumors. In: Yalcin S, Öberg K, eds. *Neuroendocrine Tumours: Diagnosis and Management*. Berlin: Springer; 2015:23-33.
3. Sackstein PE, O'Neil DS, Neugut AI, Chabot J, Fojo T. Epidemiologic trends in neuroendocrine tumors: an examination of incidence rates and survival of specific patient subgroups over the past 20 years. *Semin Oncol*. 2018;45:249-258.
4. Chauhan A, Yu Q, Ray N, et al. Global burden of neuroendocrine tumors and changing incidence in Kentucky. *Oncotarget*. 2018;9:19245-19254.
5. Oronsky B, Ma PC, Morgensztern D, Carter CA. Nothing But NET: a review of neuroendocrine tumors and carcinomas. *Neoplasia*. 2017;19:991-1002.
6. Cloyd JM. Non-functional neuroendocrine tumors of the pancreas: advances in diagnosis and management. *World J Gastroenterol*. 2015;21:9512.
7. Halfdanarson TR, Rabe KG, Rubin J, Petersen GM. Pancreatic neuroendocrine tumors (PNETs): incidence, prognosis and recent trend toward improved survival. *Ann Oncol*. 2008;19:1727-1733.
8. Nagtegaal ID, Odze RD, Klimstra D, et al. The 2019 WHO classification of tumours of the digestive system. *Histopathology*. 2020;76:182-188.
9. Keutgen XM, Nilubol N, Glanville J, et al. Resection of primary tumor site is associated with prolonged survival in metastatic nonfunctioning pancreatic neuroendocrine tumors. *Surgery*. 2016;159:311-318.
10. Sanli Y, Garg I, Kandathil A, et al. Neuroendocrine tumor diagnosis and management: 68Ga-DOTATATE PET/CT. *Am J Roentgenol*. 2018;211:267-277.
11. Sundin A. Novel functional imaging of neuroendocrine tumors. *Endocrinol Metab Clin North Am*. 2018;47:505-523.
12. Yang J, Kan Y, Ge BH, Yuan L, Li C, Zhao W. Diagnostic role of Gallium-68 DOTATOC and Gallium-68 DOTATATE PET in patients with neuroendocrine tumors: a meta-analysis. *Acta Radiol*. 2014;55:389-398.

13. Johnbeck CB, Knigge U, Kjær A. PET tracers for somatostatin receptor imaging of neuroendocrine tumors: current status and review of the literature. *Future Oncol*. 2014;10:2259-2277.
14. Geijer H, Breimer LH. Somatostatin receptor PET/CT in neuroendocrine tumours: update on systematic review and meta-analysis. *Eur J Nucl Med Mol Imaging*. 2013;40:1770-1780.
15. Treglia G, Castaldi P, Rindi G, Giordano A, Rufini V. Diagnostic performance of Gallium-68 somatostatin receptor PET and PET/CT in patients with thoracic and gastroenteropancreatic neuroendocrine tumours: a meta-analysis. *Endocrine*. 2012;42:80-87.
16. Graham MM, Gu X, Ginader T, Breheny P, Sunderland JJ. 68Ga-DOTATOC imaging of neuroendocrine tumors: a systematic review and metaanalysis. *J Nucl Med*. 2017;58:1452-1458.
17. Sundin A, Arnold R, Baudin E, et al. ENETS consensus guidelines for the standards of care in neuroendocrine tumors: radiological, nuclear medicine and hybrid imaging. *Neuroendocrinology*. 2017;105:212-244.
18. Gabriel M, Decristoforo C, Kendler D, et al. 68Ga-DOTA-Tyr3-Octreotide PET in neuroendocrine tumors: comparison with somatostatin receptor scintigraphy and CT. *J Nucl Med*. 2007;48:508-518.
19. Mayerhoefer ME, Prosch H, Beer L, et al. PET/MRI versus PET/CT in oncology: a prospective single-center study of 330 examinations focusing on implications for patient management and cost considerations. *Eur J Nucl Med Mol Imaging*. 2020;47:51-60.
20. Messina C, Bignone R, Bruno A, et al. Diffusion-weighted imaging in oncology: an update. *Cancers*. 2020;12:1493.
21. Vilgrain V, Esvan M, Ronot M, Caumont-Prim A, Aubé C, Chatellier G. A meta-analysis of diffusion-weighted and gadoxetic acid-enhanced MR imaging for the detection of liver metastases. *Eur Radiol*. 2016;26:4595-4615.
22. Mayerhoefer ME, Ba-Ssalamah A, Weber M, et al. Gadoxetate-enhanced versus diffusion-weighted MRI for fused Ga-68-DOTANOC PET/MRI in patients with neuroendocrine tumours of the upper abdomen. *Eur Radiol*. 2013;23:1978-1985.
23. Kulke MH, Anthony LB, Bushnell DL, et al. NANETS treatment guidelines. *Pancreas*. 2010;39:735-752.
24. Orlefors H, Sundin A, Garske U, et al. Whole-body (11)C-5-hydroxytryptophan positron emission tomography as a universal imaging technique for neuroendocrine tumors: comparison with somatostatin receptor scintigraphy and computed tomography. *J Clin Endocrinol Metab*. 2005;90:3392-3400.
25. Orlefors H, Sundin A, Ahlström H, et al. Positron emission tomography with 5-hydroxytryprophan in neuroendocrine tumors. *JCO*. 1998;16:2534-2541.
26. Bjurling P, Antoni G, Watanabe Y, et al. Enzymatic synthesis of carboxy-11C-labelled L-tyrosine, L-DOPA, L-tryptophan and 5-Hydroxy-L-tryptophan. *Acta Chem Scand*. 1990;44:178-182.
27. Orlefors H, Sundin A, Lu L, et al. Carbidopa pretreatment improves image interpretation and visualisation of carcinoid tumours with 11C-5-hydroxytryptophan positron emission tomography. *Eur J Nucl Med Mol Imaging*. 2006;33:60-65.
28. Sawicki LM, Deuschl C, Beiderwellen K, et al. Evaluation of 68Ga-DOTATOC PET/MRI for whole-body staging of neuroendocrine tumours in comparison with 68Ga-DOTATOC PET/CT. *Eur Radiol*. 2017;27:4091-4099.
29. Beiderwellen KJ, Poeppel TD, Hartung-Knemeyer V, et al. Simultaneous 68Ga-DOTATOC PET/MRI in patients with gastroenteropancreatic neuroendocrine tumors: initial results. *Invest Radiol*. 2013;48:273-279.
30. Hope TA, Pampaloni MH, Nakakura E, et al. Simultaneous 68Ga-DOTA-TOC PET/MRI with gadoxetate disodium in patients with neuroendocrine tumor. *Abdom Imaging*. 2015;40:1432-1440.
31. Berzaczy D, Giraudo C, Haug AR, et al. Whole-Body 68Ga-DOTANOC PET/MRI versus 68Ga-DOTANOC PET/CT in patients with neuroendocrine tumors. *Clin Nucl Med*. 2017;42:669-674.
32. Ruf J, Schiefer J, Furth C, et al. 68Ga-DOTATOC PET/CT of neuroendocrine tumors: spotlight on the CT phases of a triple-phase protocol. *J Nucl Med*. 2011;52:697-704.
33. Schraml C, Schwenzer NF, Sperling O, et al. Staging of neuroendocrine tumours: comparison of [68Ga]DOTATOC multiphase PET/CT and whole-body MRI. *Cancer Imaging*. 2013;13:63-72.
34. Örlefors H, Sundin A, Eriksson B, et al. PET-guided surgery — High correlation between positron emission tomography with 11C-5-Hydroxytryptophane (5-HTP) and surgical findings in abdominal neuroendocrine tumours. *Cancers (Basel)*. 2012;4:100-112.
35. Koopmans KP, Neels OC, Kema IP, et al. Improved staging of patients with carcinoid and islet cell tumors with 18F-dihydroxyphenyl-alanine and 11C-5-hydroxy-tryptophan positron emission tomography. *J Clin Oncol*. 2008;26:1489-1495.
36. Ronot M, Clift AK, Baum RP, et al. Morphological and functional imaging for detecting and assessing the resectability of neuroendocrine liver metastases. *Neuroendocrinology*. 2018;106:74-88.
37. Giesel FL, Kratochwil C, Mehndiratta A, et al. Comparison of neuroendocrine tumor detection and characterization using DOTATOC-PET in correlation with contrast enhanced CT and delayed contrast enhanced MRI. *Eur J Radiol*. 2012;81:2820-2825.
38. Putzer D, Gabriel M, Henninger B, et al. Bone metastases in patients with neuroendocrine tumor: 68Ga-DOTA-Tyr3-octreotide PET in comparison to CT and bone scintigraphy. *J Nucl Med*. 2009;50:1214-1221.
39. Seith F, Schraml C, Reischl G, et al. Fast non-enhanced abdominal examination protocols in PET/MRI for patients with neuroendocrine tumors (NET): comparison to multiphase contrast-enhanced PET/CT. *Radiol med*. 2018;123:860-870.
40. Altieri B, Di Dato C, Martini C, et al. Bone Metastases in neuroendocrine neoplasms: from pathogenesis to clinical management. *Cancers (Basel)*. 2019;11:1332.
41. Scharf M, Petry V, Daniel H, Rinke A, Gress TM. Bone metastases in patients with neuroendocrine neoplasm: frequency and clinical, therapeutic, and prognostic relevance. *Neuroendocrinology*. 2018;106:30-37.
42. Albanus DR, Apitzsch J, Erdem Z, et al. Clinical value of 68Ga-DOTATATE-PET/CT compared to stand-alone contrast enhanced CT for the detection of extra-hepatic metastases in patients with neuroendocrine tumours (NET). *Eur J Radiol*. 2015;84:1866-1872.
43. Ambrosini V, Nanni C, Zompatori M, et al. (68)Ga-DOTA-NOC PET/CT in comparison with CT for the detection of bone metastasis in patients with neuroendocrine tumours. *Eur J Nucl Med Mol Imaging*. 2010;37:722-727.
44. Kos-Kudła B, O'Toole D, Falconi M, et al. ENETS consensus guidelines for the management of bone and lung metastases from neuroendocrine tumors. *Neuroendocrinology*. 2010;91:341-350.
45. Stecco A, Trisoglio A, Soligo E, Berardo S, Sukhovei L, Carriero A. Whole-body MRI with diffusion-weighted imaging in bone metastases. a narrative review. *Diagnostics (Basel)*. 2018;8:45.
46. Coakley FV, Choi PH, Gougoutas CA, et al. Peritoneal metastases: detection with spiral CT in patients with ovarian cancer. *Radiology*. 2002;223:495-499.
47. Low RN, Barone RM, Lucero J. Comparison of MRI and CT for predicting the Peritoneal Cancer Index (PCI) preoperatively in patients being considered for cytoreductive surgical procedures. *Ann Surg Oncol*. 2015;22:1708-1715.
48. Norlén O, Montan H, Hellman P, Stålberg P, Sundin A. Preoperative 68Ga-DOTA-somatostatin analog-PET/CT hybrid imaging increases detection rate of intra-abdominal small intestinal neuroendocrine tumor lesions. *World J Surg*. 2018;42:498-505.

How to cite this article: Jawlakh H, Velikyan I, Welin S, Sundin A. ^{68}Ga-DOTATOC-PET/MRI and ^{11}C-5-HTP-PET/MRI are superior to ^{68}Ga-DOTATOC-PET/CT for neuroendocrine tumor imaging. *J Neuroendocrinol*. 2021;33:e12981. https://doi.org/10.1111/jne.12981